Meter is the path of length that light passes in vacuum for the time interval equal to 1/299752498 s. The speed of light is equal to 299792458 m/s (exactly). (1/10 000 000 part of meridian from the equator to the North Pole)

Second is defined by using the Cesium clock (laser). Second is the time equal to 9192631770 periods of radiation corresponding to transition between two hyperfine levels of the ^{133}Cs ground state atom. $(1/(24 \cdot 60 \cdot 60)$ part of the Sun day)

Electric voltage U may be measured by using the nonstationary Josepson effect, where $h\omega = 2e \cdot U$, at that ω is measured by using the Cesium clock.

Electrical resistance R should be expressed in the units of quantum electrical resistance R_K by using the quantum Hall effect; $R_K = h/e^2 = 25812.807557(18)\ \Omega$ is the von Kleitzing constant. In the Hall effect $R = U_{trans}/I_{long}$.

... etc.

ISOMERIC STATE IN ^{229}Th AND IT'S POPULATION IN THE REACTION OF THE COULOMB EXCITATION

V. I. Isakov

Petersburg Nuclear Physics Institute, NRC Kurchatov Institute, 188300 Gatchina, Russia

On the basis of detailed analysis of γ-transitions in ^{229}Th attendant α-decay of ^{233}U, it was established the existence in the daughter nuclei ^{229}Th of the low-lying level with the excitation energy of only a few eV. This is the most low-lying state known by now. The next one is the level $1/2^+$ in ^{235}U, with the excitation energy equal to 76.5 eV. The latest experimental data point to the value of the excitation energy in $^{229}_{90}\mathrm{Th}_{139}$ equal to $\sim$ 7.6 eV. Not long ago, conversion electrons arising from the decay of this level were also detected, their energies were not defined. In this way, it was proved that this level really exists, and it's energy is above the threshold of ionization of neutral atom of Th, which is equal to $\sim$ 6.1 eV. Together, the half-life of this level equal to $7(\pm1)$ μs was measured recently. However, the energy of this state is not yet measured in the direct experiment.

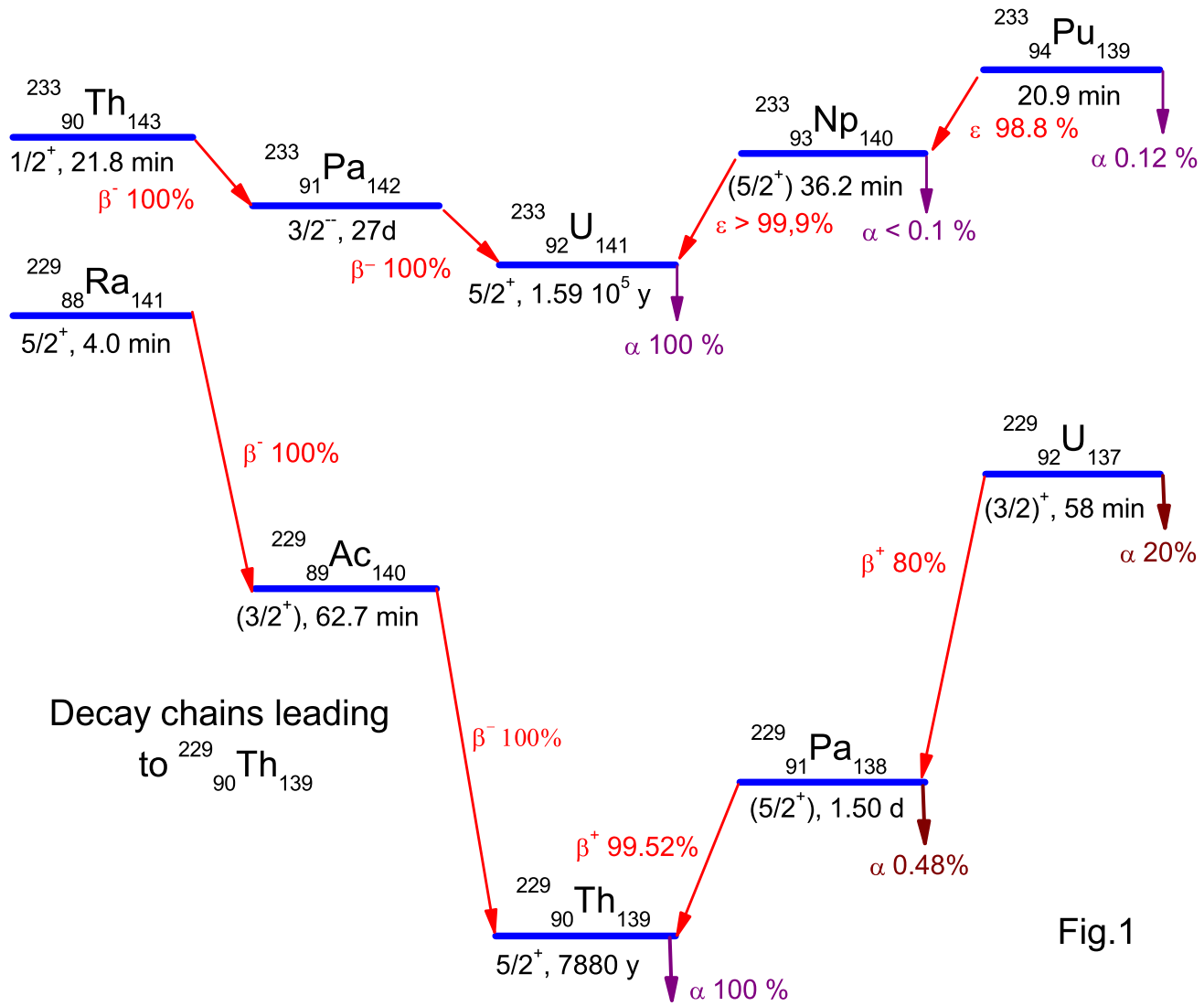

Figure 1: Chain of decays leading to ^{229}Th

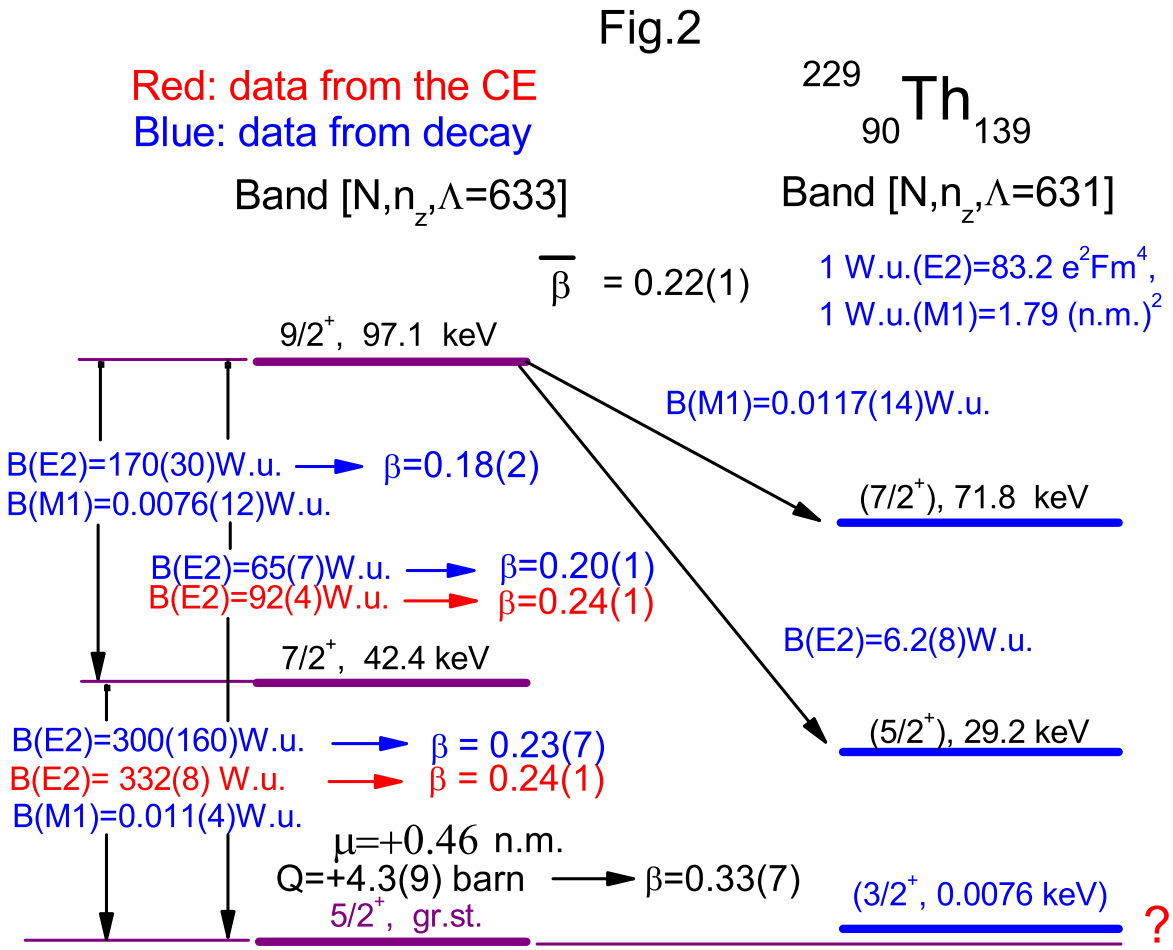

Experimental data are from E. Browne and J.K. Tuli, NDS v. 109, 2657 (2008). Data on the Coulomb excitation of the $9/2^+$, 97.1 and $7/2^+$, 42.4 keV levels were also obtained in the paper of S.J. Goldstein et.al. Phys.Rev. C40, 2793 (1989).

Figure 2: Low-lying levels in ^{229}Th

The wave function of the axially-symmetric odd nuclei in the framework of the unified model reads as

$$\Psi^J_{MK} \;=\; \sqrt{\frac{\overline{2J+1}}{16\pi^2}}\Big[D^J_{MK}(\theta_i)\cdot\chi_K + D^J_{M-K}(\theta_i)\cdot\overline{\chi^J_K}\Big]\,. \tag{1}$$

Second term in (1) provides symmetry of the wave function to reflection relatively the plane orthogonal to the symmetry axis, while

$$\chi_K = \sum_{N\ell\Lambda s} x_K(N\ell\Lambda s)|N\ell\Lambda s\rangle\,, \quad \overline{\chi^J_K} = \sum_{N\ell\Lambda s}(-1)^{J-\ell-1/2}x_K(N\ell\Lambda s)|N\ell-\Lambda-s\rangle\,. \tag{2}$$

In (1) and (2) χ_K are Nilsson orbitals, that represent the decomposition of the single-particle functions of the axially-symmetric deformed potential over the spherical-symmetric functions, Λ and s are projections of orbital moment and spin on the symmetry axis, $K=\Lambda+s$.

We define reduced transition matrix elements and reduced transition rates by the relations

$$\langle J_2M_2|\hat m(\lambda\mu)|J_1M_1\rangle \;=\; (-1)^{J_2-M_2}\begin{pmatrix} J_2 & \lambda & J_1\\ -M_2 & \mu & M_1\end{pmatrix}\langle J_2\|\hat m(\lambda)\|J_1\rangle\,,$$

$$\langle J_2\|\hat m(\lambda)\|J_1\rangle = (-1)^{J_2-J_1}\langle J_1\|\hat m(\lambda)\|J_2\rangle\,. \tag{3}$$

$$B(\lambda;J_1\to J_2) = \frac{\langle J_2\|\hat m(\lambda)\|J_1\rangle^2}{2J_1+1}\,,\;\; B(\lambda;J_1\to J_2) = \frac{2J_2+1}{2J_1+1}B(\lambda;J_2\to J_1)\,. \tag{4}$$

For $E2$ transitions we have

$$\hat{m}(E2,core)^2_\mu = D^2_{\mu 0}(\theta_i)\cdot\frac{3}{4\pi}ZR^2\cdot\beta|e|,\ \text{while}\ \ \hat{m}(E2,s.p.)^2_\mu = \sum_\nu D^2_{\mu\nu}(\theta_i)\cdot\hat{m}(E2,intr.)^2_\nu\,. \quad (5)$$

Then, we obtain

$$\begin{aligned}
&\langle\Psi^{J_2}_{K_2}\,\|\hat{m}(E2,core)+\hat{m}(E2,s.p.)\|\Psi^{J_1}_{K_1}\rangle\ =\\
&=\quad (-1)^{J_2-J_1}\sqrt{\overline{(2J_1+1)}}\,C^{J_2K_2}_{20\,J_1K_1}\delta(K_1,K_2)\delta(\alpha_1,\alpha_2)\,\frac{3}{4\pi}\,|e|\cdot ZR^2\cdot\beta\ +\\
&+\quad (-1)^{J_2-J_1}\sqrt{\frac{\overline{5(2J_1+1)}}{4\pi}}\cdot\sum_{N\ell\Lambda(1,2)}x_{K_2}(N_2\ell_2\Lambda_2 s_2)\,x_{K_1}(N_1\ell_1\Lambda_1 s_1)\,.(u_{K_1}u_{K_2}-v_{K_1}v_{K_2})\ \times\\
&\times\quad\sqrt{\frac{\overline{2\ell_1+1}}{2\ell_2+1}}C^{\ell_2 0}_{20\ell_1 0}\Big[\delta(s_1,s_2)C^{J_2K_2}_{2(K_2-K_1)J_1K_1}C^{\ell_2\Lambda_2}_{2(K_2-K_1)\ell_1\Lambda_1}\ +\\
&+\quad\delta(s_1,-s_2)(-1)^{J_2-\ell_2-1/2}C^{J_2-K_2}_{2(-K_2-K_1)J_1K_1}C^{\ell_2-\Lambda_2}_{2(-K_2-K_1)\ell_1\Lambda_1}\Big]\ \cdot e_{\text{eff}}\cdot\langle 2|r^2|1\rangle\,. \qquad (6)
\end{aligned}$$

In (6) u and v are the coefficients of the Bogoliubov transformation, that accounts the superfluid correlations, while e_{eff} is the effective quadrupole charge for the odd particle.

Quadrupole moment of state is expressed via the reduced $E2$ matrix elements by the relation

$$Q_2(J) \;=\; \sqrt{\frac{16\pi\, J(2J-1)}{5(J+1)(2J+1)(2J+3)}}\;\langle\, J\|\hat{m}(E2)\|J\,\rangle\,. \tag{7}$$

Consider now $M1$ transitions. Because of the particle-hole polarization arising from the spin-dependent interactions between the nucleons, "bare" values of gyromagnetic ratios in nuclei renormalize. In addition, this polarization leads to the appearance of the additional tensor term in the single-particle $M1$ operator which "opens" l-forbidden transitions in spherical nuclei. In this way, the $M1$ transition operator in our case reads as

$$\hat{m}(M1)^1_\mu \;=\; \sqrt{\frac{3}{4\pi}}\,\mu_N\left[g_R\hat{J}+(g_\ell-g_R)\hat{\ell}+(g_s-g_R)\hat{s}+\delta\hat{\mu}(M1,tens.)\right]^1_\mu, \tag{8}$$

$$\text{where}\;\; \delta\hat{\mu}(M1,tens.)^1_\mu \;=\; \kappa r^2[Y_2\otimes\hat{s}]^1_\mu\cdot\tau_3\,. \tag{9}$$

In (9) $\tau_3=+1$ for neutrons (n) and $\tau_3=-1$ for protons (p); $\kappa=-0.031$ fm^{-2}; $g_\ell(p)\approx 1.1$, $g_\ell(n)\approx 0.0$, $g_s(p)=3.79$, $g_s(n)=-2.04$, $g_R=Z/A=90/229=0.393$. The values of parameters g_l, g_s and κ were defined by us before from the description of magnetic moments as well as l-allowed and l-forbidden $M1$ transition rates in spherical nuclei, both near and far from the closed shells. As a result, we obtain the formula for the reduced $M1$ transition matrix element:

$$\langle\Psi^{J_2}_{K_2}\|\hat{m}(M1,core)+\hat{m}(M1,s.p.)\|\Psi^{J_1}_{K_1}\rangle \;=$$

$$
\begin{aligned}
= \quad & g_R\ \mu_N\, \delta(K_1,K_2)\delta(J_1,J_2)\delta(\alpha_1,\alpha_2)\sqrt{\frac{3J_1(J_1+1)(2J_1+1)}{4\pi}}\ + \\
& + (-1)^{J_2-J_1}\sqrt{\frac{3(2J_1+1)}{4\pi}}\,\mu_N \sum_{N\ell\Lambda s(1,2)} x_{K_2}(N_2\ell_2\Lambda_2 s_2)x_{K_1}(N_1\ell_1\Lambda_1 s_1)\,.(u_{K1}u_{K2}+v_{K_1}v_{K_2})\ \times \\
& \times\Bigg\{ (g_\ell - g_R)\sqrt{\ell_1(\ell_1+1)}\,\delta(n_1,n_2)\delta(\ell_1,\ell_2)\Big[\delta(s_1,s_2)C^{J_2K_2}_{1(K_2-K_1)J_1K_1}\ \times \\
& \times\ C^{\ell_2\Lambda_2}_{1(K_2-K_1)\ell_1\Lambda_1} + \delta(s_1-s_2)(-1)^{J_2-\ell_2-1/2}C^{J_2-K_2}_{1(-K_2-K_2)J_1K_1}C^{\ell_2-\Lambda_2}_{1(-K_2-K_1)\ell_1\Lambda_1}\Big]\ + \\
& + (g_s-g_R)\frac{\sqrt{3}}{2}\,\delta(n_1,n_2)\delta(\ell_1\ell_2)\Big[\delta(\Lambda_1,\Lambda_2)C^{J_2K_2}_{1(K_2-K_1)J_1K_1}C^{1/2\,s_2}_{1(K_2-K_1)1/2\,s_1}\ + \\
& +\quad \delta(\Lambda_1,-\Lambda_2)(-1)^{J_2-\ell_2-1/2}C^{J_2-K_2}_{1(-K_2-K_1)J_1K_1}C^{1/2-s_2}_{1(-K_2-K_1)1/2\,s_1}\Big]\ - \\
& - \kappa\langle 2|r^2|1\rangle\Big[C^{J_2K_2}_{1(K_2-K_1)J_1K_1}\langle\ell_2\Lambda_2 1/2\,s_2|[Y_2\otimes\hat{s}]^1_{(K_2-K_1)}\,|\ell_1\Lambda_1 1/2\,s_1\rangle\ + \\
& +(-1)^{J_2-\ell_2-1/2}C^{J_2-K_2}_{1(-K_2-K_1)J_1K_1}\langle\ell_2-\Lambda_2 1/2-s_2|[Y_2\otimes\hat{s}]^1_{(-K_2-K_1)}|\ell_1\Lambda_1 1/2\,s_1\rangle\Big]\Bigg\}.
\end{aligned}
\tag{10}
$$

Here, $K_1 = \Lambda_1 + s_1$, $K_2 = \Lambda_2 + s_2$, while

$$\langle\, \ell_2 \Lambda_2 1/2\, s_2 | [Y_2 \otimes \hat{s}]^1_\mu \,| \ell_1 \Lambda_1 1/2\, s_1]\,\rangle \;=\; \frac{3}{2}\sqrt{\frac{5(2\ell_1+1)}{2\pi}}\, C^{\ell_2 0}_{\ell_1 0\, 2\, 0} \;\times$$

$$\times \sum_{j_1 j_2} \sqrt{(2j_1+1)} C^{j_2 K_2}_{j_1 K_1 1 \mu} C^{j_2 K_2}_{\ell_2 \Lambda_2 1/2 s_2} C^{j_1 K_1}_{\ell_1 \Lambda_1 1/2 s_1} \left\{ \begin{array}{ccc} \ell_2 & 1/2 & j_2 \\ \ell_1 & 1/2 & j_1 \\ 2 & 1 & 1 \end{array} \right\}, \mu = \Lambda_2 + s_2 - \Lambda_1 - s_1 \quad (11)$$

Magnetic moments of states are defined by the relation

$$\mu_J \;=\; \sqrt{\frac{4\pi J}{3(J+1)(2J+1)}}\, \langle\, J \| \hat{m}(M1) \| J \,\rangle\,. \quad (12)$$

For the $E2$ transitions between the states of the same rotational band, we may in formula (6) take into account only collective part of the matrix element, as the single-particle one gives only a small contribution. Then, we have formulas for the quadrupole moments of states and for the transition rates, where the result depends only on the deformation parameter β and the entering values of J and K:

$$Q_2(J,K)=\frac{3K^2-J(J+1)}{(J+1)(2J+3)}\,Q_0;\;\; Q_2(K=J)=\frac{J(2J-1)}{(J+1)(2J+3)}\,Q_0\,;\; Q_0\;=\frac{3}{\sqrt{5\pi}}|e|ZR^2\cdot\beta. \tag{13}$$

$$B(E2;\,J+1,K\to J,K)\;=\;\frac{3K^2(J+1+K)(J+1-K)}{J(J+1)(J+2)(2J+3)}\cdot\frac{5}{16\pi}\,Q_0^2\,, \tag{14}$$

$$B(E2;\,J+2,K\to J,K)\;=\;\frac{3(J+2+K)(J+1+K)(J+2-K)(J+1-K)}{(2J+2)(2J+3)(J+2)(2J+5)}\cdot\frac{5}{16\pi}\,Q_0^2\,. \tag{15}$$

By using experimental data shown in Fig.2 and formulas (13)–(15), one can easily define the magnitude of the deformation parameter β which average value turns out to be $\overline{\beta}\approx 0.22$. This is close to the magnitude of β, that corresponds to maximal value of the binding energy B in ^{229}Th obtained in calculations, which were performed in the Hartree–Fock–Bogoliubov approach with the Gogny interaction. This value of β was used by us in our calculations that involve the "intrinsic" function χ. Mention, that both collective and single-particle parts in the $M1$ transition matrix element (10) give comparable contributions even in case of transitions within the same rotational band.

Consider now transitions between the states of different bands $|(J_1,J_1^{'})K_1\rangle\to|(J_2,J_2^{'})K_2\rangle$, where the initial as well as final states have different values of $(J,J^{'})$, but the same values of K. We see from formula (6) that in case of the $E2$-transitions matrix element contains the multiple $(u_{K_1}u_{K_2}-v_{K_1}v_{K_2})$, which value

is very sensitive to small variation of the single-particle scheme, especially when the entering single-particle orbitals are close to the Fermi level. This is just the case under consideration. In addition, the value of the effective quadrupole charge $e_{\rm eff}$ is rather indefinite here, as it is not clear, what part of the quadrupole transition strength should be included in the single-particle mode after taking into account rotation of the core in the obvious way. Thus, direct calculations of the $E2$ transition matrix elements are not trustworthy here. However, one can easily see from formulas (6) and (10), that if the multipolarity of radiation λ satisfies the condition $K_1 + K_2 > \lambda$, as it takes place if we consider $E2$ and $M1$ trasitions between the bands $[633]$ and $[631]$, then we have the relation

$$B(\lambda; J_1' K_1 \to J_2' K_2) = \frac{[C^{J_2' K_2}_{\lambda(K_2-K_1)J_1' K_1}]^2}{[C^{J_2 K_2}_{\lambda(K_2-K_1)J_1 K_1}]^2} B(\lambda; J_1 K_1 \to J_2 K_2). \qquad (16)$$

As we know from the experiment the value of $B(E2; J_1 = 9/2, K_1 = 5/2 \to J_2 = 5/2, K_2 = 3/2)$ $= 6.2(8)$ W.u., we can define in this way all interband $E2$-transition matrix elements.

The situation is different in case of $M1$ transitions. Here, both collective and single-particle parts of the $M1$ transition matrix element (10) give comparable contributions even in cases of transitions within the same rotational band. In this case, multiple $(u_{K_1} u_{K_2} + v_{K_1} v_{K_2})$ is close to unity, while the values of g_s and κ are known. Thus, calculations of $M1$ transition matrix elements were performed in the obvious way, both for interband transitions and for transitions within the same band.

Table 1: Reduced transition rates for the interband $E2$ and $M1$ transitions between the low-lying levels of the bands $[N_1 n_z(1)\Lambda_1] = [633]$ and $[N_2 n_z(2)\Lambda_2] = [631]$ in ^{229}Th. Calculations of the $E2$ transition rates, shown in the W.u., were based on formula (16), where the experimental value of $B(E2; J_1 = 9/2\, K_1 = 5/2\, [633] \rightarrow J_2 = 5/2\, K_2 = 3/2\, [631]) = 6.2(8)$ was used as the normalization factor. Here, W.u.$(E2)$ =83.2 e^2fm^4. Results on the $B(M1)$ values are shown in the units of μ_N^2 (1 W.u.$(M1) = 1.79\ \mu_N^2$), and they were obtained by calculations basing on formula (10) with $\beta = 0.2$, $g_s(n, \mathrm{eff}) = -2,04$ and $\kappa = -0.031$ fm^{-2}.

$E, M(\lambda)$	$J_1\, K_1$	$J_2\, K_2$	$B(1 \rightarrow 2)$	$E, M(\lambda)$	$J_1\, K_1$	$J_2\, K_2$	$B(1 \rightarrow 2)$
$E2$	9/2 3/2	5/2 5/2	0.53	$E2$	3/2 3/2	5/2 5/2	8.0
$E2$	9/2 3/2	7/2 5/2	4.6	$M1$	9/2 3/2	7/2 5/2	0.00072
$E2$	9/2 3/2	9/2 5/2	3.9	$M1$	9/2 3/2	9/2 5/2	0.00460
$E2$	9/2 5/2	5/2 3/2	6.2 [6.2(8)]	$M1$	9/2 5/2	7/2 3/2	0.00506 [0.0209(25)]
$E2$	9/2 5/2	7/2 3/2	0.11	$M1$	7/2 3/2	5/2 5/2	0.00039
$E2$	7/2 3/2	5/2 5/2	3.3	$M1$	7/2 3/2	7/2 5/2	0.00413
$E2$	7/2 3/2	7/2 5/2	5.7	$M1$	7/2 5/2	5/2 3/2	0.00581
$E2$	7/2 5/2	3/2 3/2	5.3	$M1$	5/2 3/2	5/2 5/2	0.00310
$E2$	7/2 5/2	5/2 3/2	0.22	$M1$	3/2 3/2	5/2 5/2	0.01080
$E2$	5/2 3/2	5/2 5/2	8.0				

Table 2: Reduced $E2$ and $M1$ transition rates between the levels inside the $K = 5/2$ and $K = 3/2$ bands. Here, the $B(E2)$ values are in the Weisskopf units and were calculated by using $\overline{\beta} = 0.22$. Numbers in square brackets show experimental results. The M1 rates are in the units of μ_N^2, and they were calculated by using $g_s(n, \mathrm{eff}) = -2.04$ and $\kappa = -0.031\,\mathrm{fm}^{-2}$.

$E, M(\lambda)$	$J_1\,K_1$	$J_2\,K_2$	$B(1 \to 2)$	$E, M(\lambda)$	$J_1\,K_1$	$J_2\,K_2$	$B(1 \to 2)$
$E2$	9/2 3/2	5/2 3/2	167	$E2$	5/2 3/2	3/2 3/2	267
$E2$	9/2 3/2	7/2 3/2	109	$M1$	9/2 3/2	7/2 3/2	0.0583
$E2$	9/2 5/2	5/2 5/2	78 [85(4)]	$M1$	9/2 5/2	7/2 5/2	0.0386 [0.0136(21)]
$E2$	9/2 5/2	7/2 5/2	236 [170(30)]	$M1$	7/2 3/2	5/2 3/2	0.0521
$E2$	7/2 3/2	3/2 3/2	111	$M1$	7/2 5/2	5/2 5/2	0.0266 [0.0197(72)]
$E2$	7/2 3/2	5/2 3/2	167	$M1$	5/2 3/2	3/2 3/2	0.0389
$E2$	7/2 5/2	5/2 5/2	279 [330(8)]				

Table 3: Electric quadrupole and magnetic dipole moments of the lowest states of ^{229}Th. Here, by calculation of quadrupole moments we used averaged value of $\overline{\beta}$ =0.22, while by calculation of magnetic moments we used $\beta = 0.2$, $g_s(n, \mathrm{eff}) = -2.04$ and $\kappa = -0.031\,\mathrm{fm}^{-2}$.

Quantity(J , K)	Exp.	Calc.	Quantity(J , K)	Exp.	Calc.
$Q_2(5/2\,, 5/2)$	+4.3(9) barn	+2.9 barn	$Q_2(3/2\,, 3/2)$	–	+1.6 barn
$\mu(5/2\,, 5/2)$	+0.46(4) μ_N	$+0.47\,\mu_N$	$\mu(3/2\,, 3/2)$	–	$+0.12\,\mu_N$

By using data on transition rates shown in Table 1, $B(M1; 3/2, 3/2 \to 5/2, 5/2) = 0.0108\,\mu_N^2$ and $B(E2; 3/2, 3/2 \to 5/2, 5/2) = 8.0$ W.u., and the values of the conversion coefficients for the 0.0076 keV γ-transition (private communication of M.B. Trzhaskovskaya), we find the half-lives for this transition equal to $T_{1/2}(M1) = 5.9 \cdot 10^{-6}$ s and $T_{1/2}(E2) = 2.7 \cdot 10^{-3}$ s (including electron conversion). Experimental value of $T_{1/2}$ is $7 \pm 1 \cdot 10^{-6}$ s. Here, conversion coefficients are very large: $\alpha_{tot}^{M1}(0.0076\ \mathrm{keV}) \approx 1.4 \cdot 10^9$ and $\alpha_{tot}^{E2}(0.0076\ \mathrm{keV}) \approx 1.2 \cdot 10^{16}$. It is important that at such small transition energies, conversion coefficients rapidly grow with decrease of the transition energy (approximately, for $\Delta E \leq 20$ eV, $\alpha_{tot}^{M1} \sim 1/(\Delta E)^{3-\epsilon}$ and $\alpha_{tot}^{E2} \sim 1/(\Delta E)^{5-\epsilon}$, where $\epsilon \sim 0.05$). *As a result, the half-life of the state of interest at such small transition energies in practice does not depend on energy, but only on the transition matrix element*.

Below, we discuss the problem of population of the above-mentioned isomeric state by the method different from α and β-decays. Some authors proposed the method which employs synchrotron radiation, while other ones suggested pumping ^{229m}Th by the hollow-cathode discharge. These attempts gave no result. Here, we consider the chance for excitation of the isomeric state in the Coulomb excitation, the process that was proposed for the first time by K.A. Ter-Martirosyan.

For the $E2$ Coulomb excitation we have

$$\frac{d\sigma_{E2}(\xi,\vartheta)}{d\,\Omega} = \left(\frac{Z_1 e^2}{\hbar v}\right)^2 \frac{1}{a^2}\, B(E2\uparrow)\frac{df_{E2}(\xi,\vartheta)}{d\Omega}\,,$$

$$a \approx 0.072\,\frac{Z_1 Z_2}{E_1(\mathrm{MeV})}(1+A_1/A_2)\cdot 10^{-12}\mathrm{cm}\,,\ \xi = \frac{Z_1 Z_2 A_1^{1/2}(1+A_1/A_2)\Delta E}{12.65(E_1 - 1/2\cdot\Delta E)^{3/2}}\,. \qquad (17)$$

Here, A_1, Z_1 and E_1 refer to the projectile, E_1 and ΔE are energy in the laboratory system and the excitation energy in MeV, a is half the distance of the closest drawing in the backward scattering. Functions $f_{E2}(\xi,\vartheta)$ are expressed via integrals over trajectories. If $\Delta E/E_1 = 0$, then we obtain

$$\frac{df_{E2}(\xi=0,\vartheta)}{d\,\Omega} \;=\; \frac{\pi}{25}\left\{\left[1-\frac{\pi-\vartheta}{2}\tan\frac{\vartheta}{2}\right]^2\cdot\frac{1}{\cos^4\vartheta/2}+\frac{1}{3}\right\}. \qquad (18)$$

In a general case, we have

$$\sigma_{E2}(\xi) \;\approx\; 4.78\,\frac{A_1 E_{kin}(A_1,\mathrm{MeV})B(E2\uparrow,\mathrm{barn}^2)}{Z_2^2(1+A_1/A_2)^2} f_{E2}(\xi)\ \mathrm{barn}, \tag{19}$$

where $f_{E2}(\xi=0)=0.895$.

For the $M1$ Coulomb excitation we have

$$\frac{d\sigma_{M1}(\xi,\vartheta)}{d\,\Omega} = \left(\frac{Z_1 e^2}{\hbar c}\right)^2 \frac{\lambda\!\!\!^{-}_c\,(p)^2}{4}\, B(M1\uparrow)\frac{df_{M1}(\xi,\vartheta)}{d\,\Omega}\,, \quad \lambda\!\!\!^{-}_c\,(p) = \frac{\hbar}{m_p c}\,. \tag{20}$$

For $\xi=0$ we obtain

$$\frac{df_{M1}(\xi=0,\vartheta)}{d\,\Omega} \;=\; \frac{16\pi}{9}\,\frac{\left[1-(\pi-\vartheta)/2\,\cdot\,\tan\vartheta/2\right]^2}{\sin^2\vartheta}\,. \tag{21}$$

We see from Eq.(21), that by $\Delta E\to 0$ (as in our case) and $\vartheta\to 0$ the total cross section logarithmically diverges. At the same time, the probability of the $M1$ excitation by $\xi=0$, $P(M1,\xi=0,\vartheta) = d\sigma(M1,\vartheta)/d\sigma(\mathrm{Coul},\vartheta)\sim\vartheta^2$ by $\vartheta\to 0$. Thus, the divergence of the $M1$ cross section at $\vartheta\to 0$ is due only to the divergence of the Coulomb scattering at $\vartheta\to 0$, in this case the the colliding nuclei are far from each other, and the Coulomb interaction between nuclei is really screened by the electron clouds. Really, almost all electron charge of atom is located at distances less than the Bohr radius $R_B=\hbar^2/(m_e e^2)$. In this way, we should exclude intervals more than $R_{\max}$, i.e. exclude scattering angles less than $\vartheta_{\min}$, where

$$\vartheta_{\min} = 2\arcsin\left(\frac{1}{R_{\max}/a - 1}\right) \approx \frac{2a}{R_{\max}}, \quad R_{\max} \approx 2R_B\,. \tag{22}$$

Then, we obtain

$$\sigma_{M1} = 0.589 \cdot 10^{-8} Z_1^2\, B(M1\uparrow)\; f_{M1}(\xi = 0, \vartheta_{\min}) \text{ barn}\,. \tag{23}$$

Here, $B(M1)$ is in the units of μ_N^2 and

$$f_{M1}(\xi = 0, \vartheta_{\min}) \;=\; \frac{32\,\pi^2}{9} \int\limits_{\vartheta_{\min}}^{\pi} \frac{\left[1 - (\pi - \vartheta)/2 \;\cdot \tan\vartheta/2\right]^2}{\sin\vartheta}\, d\vartheta\,. \tag{24}$$

For $\vartheta_{\min\,1,2}$ less than 1^0 we have

$$f_{M1}(\xi = 0, \vartheta_{\min\,1}) \;\approx f_{M1}(\xi = 0, \vartheta_{\min\,2}) + \frac{32\pi^2}{9} \ln\left(\frac{\vartheta_{\min\,2}}{\vartheta_{\min\,1}}\right). \tag{25}$$

For protons and α-particles with energies 10 MeV bombarding ^{229}Th, $\vartheta_{min} \sim 0.1^0$ and $f_{M1}(\xi = 0, \vartheta_{min} = 0.1^0) = 186$. The corresponding cross section is negligible as compared to the $E2$ excitation, this statement is even more valid for excitation of high-lying states, for which the magnitude of f_{M1} rapidly decreases. Thus, all levels considered by us here, are populated in the Coulomb excitation by means of the $E2$ transitions.

One should allow for the fact that settlement of the lowest $3/2^+$ level may happen not only due to the direct Coulomb excitation from the ground state, but also due to the discharging of the excited higher-lying states. This process is very important as many of these states are actively excited due to large $B(E2)$ values. In this way, we took into account excitation of all levels shown in Fig. 1, as well as all possible $E2$ and $M1$ transitions between them. Corresponding $B(E2)$ and $B(M1)$ values were borrowed by us from Tables 1 and 2, while the necessary conversion coefficients were borrowed from the electronic database BRICC. Results of our calculations of cross sections are demonstrated in Table 4. Here, σ corresponds to the direct excitation, while $\sigma_{\rm eff}$ is the effective cross section, that includes settlement of the $3/2^+_1$ state by γ-transitions from the high-lying levels. One can easily see that the allowance of feeding from the high-lying states leads to considerable increase of population of the isomeric state. Note, that taking into account additional excited states leads to further increase of $\sigma_{\rm eff}$ as compared to σ.

For example, let's take the foil of ^{229}Th with thickness $d = 10\,\mu m$. The density ρ of Th is about $3 \cdot 10^{22}$ atoms/cm^3. Suppose that we have constant in time beam of 10 MeV protons with a beam current j equal to 1μA ($\sim 0.6 \cdot 10^{13}$ atoms/s).Then, the counting rate for transitions from the 0.0076 keV level (allowing also for the settlement of this level from the high-lying states that are excited in the process of the Coulomb excitation) is $N = j \cdot \sigma_{\rm eff} \cdot \rho \cdot d \approx 3 \cdot 10^5$ s^{-1}. However, this level decays mainly by the electron conversion ($\alpha^{M1}_{tot} \approx 1.4 \cdot 10^9$). Thus, the counting rate for γ-quanta is only $N_\gamma \sim 2 \cdot 10^{-4}$ s^{-1}, i.e. ~ 20 d^{-1}. However, one should keep in mind that metallic Th is not transparent for "blue" γ-rays. Thus, it is neseccary to use a target from the radiolucent glassy material containing Th atoms.

Table 4: Comparison between the cross sections σ and the "effective" cross sections $\sigma_{\rm eff}$ for the Coulomb excitation of the ^{229}Th levels by protons and α-particles.

Level	Energy keV	Protons, 6 MeV		Protons, 10 MeV		^{4}He, 10 MeV	
		σ, barn	$\sigma_{\rm eff}$, barn	σ, barn	$\sigma_{\rm eff}$, barn	σ, barn	$\sigma_{\rm eff}$, barn
$3/2^+_1$	0.0076	1.389(-4)	1.008(-3)	2.314(-4)	1.679(-3)	9.020(-4)	6.448(-3)
$5/2^+_2$	29.2	2.082(-4)	7.120(-4)	3.463(-4)	1.186(-3)	1.339(-3)	4.545(-3)
$7/2^+_1$	42.4	9.696(-3)	1.236(-2)	1.613(-2)	2.058(-2)	6.202(-2)	7.894(-2)
$7/2^+_2$	71.8	1.151(-4)	2.977(-4)	1.916(-4)	4.966(-4)	7.316 (-4)	1.890(-3)
$9/2^+_1$	97.1	3.370(-3)	3.371(-3)	5.620(-3)	5.621(-3)	2.138(-2)	2.139(-2)
$9/2^+_2$	125.4	2.291(-5)	2.291(-5)	3.831(-5)	3.831(-5)	1.429(-4)	1.429(-4)

Table 5: Gamma-transitions in nuclei with energies right up to 3 keV.

Nucleus	$T_{1/2}$ (g.s.)	E_i (keV)	J_i^π	$T_{1/2}(i)$	J_f^π	E_γ (keV)
45-V	547 ms	56.8	$(3/2-)$	0.43 μs	$(5/2-)$	0.8
90-Nb	1.46 h	124.7	4 –	18.81 s	6+	2.3
93-Tc	2.75 h	2185.16	$(17/2)-$	10.2 μs	$(17/2)+$	0.31
99-Tc	$2 \cdot 10^5$ y	142.68	$1/2-$	6.007 h	$7/2+$	2.17
110-Ag	24.5 s	1.112	2 –	660 ns	1+	1.112
154-Eu	8.6 y	100.86	4+	54 ns	3+	0.91
153-Gd	240 d	95.17	$9/2+$	3.5 μs	$7/2-$	1.83
153-Gd	240 d	171.2	$(11/2-)$	76.0 μs	$9/2-$	2.8
188-Re	17 h	172.07	(6) –	18.59 m	(3) –	2.63
186-Ir	16.6 h	$0.0 + x$	2 –	1.9 h	5+	≤ 1.5
193-Pt	50 y	1.642	$3/2-$	9.7 ns	$1/2-$	1.642
201-Hg	stable	1.565	$1/2-$	81 ns	$3/2-$	1.565
205-Pb	$1.7 \cdot 10^7$ y	2.33	$1/2-$	24.2 μs	$5/2-$	2.33
203-Po	36.7 m	641.7	$13/2+$	45 s	$7/2-$	2.1
229-Th	$7.88 \cdot 10^3$ y	0.0076	$(3/2+)$	7 μs	$5/2+$	0.0076
235- U	$7 \cdot 10^8$ y	0.076	$1/2+$	26 m	$7/2-$	0.076
250-Bk	3.2 h	35.59	$(4+)$	29 μs	$(3-)$	1.12
251-Cf	898 y	106.31	$7/2+$	38 ns	$7/2+$	0.57

^{229}Th(neutr.atom) : $T_{1/2} = 7\mu$s; $E_\gamma = 7.6$ eV; $\Delta E_\gamma(\text{rec}) = 1.35 \cdot 10^{-10}$ eV (Mossbauer)
$\Delta E_\gamma(\text{rad}) = 6.6 \cdot 10^{-11}$ eV; $\Delta E_\gamma(\text{rad})/E_\gamma = \Delta\nu/\nu = 8.7 \cdot 10^{-12}$; $\Delta\nu = 1.6 \cdot 10^4$ Hz.
$\beta(M1) \approx 1.4 \cdot 10^9; \alpha(E2) \approx 1.2 \cdot 10^{16}$.
^{229}Th (ion): I.p.(1)=6.08 eV; I.p.(2)=11.5 eV. Thus, for ^{229}Th(+) $\Delta\nu/\nu \sim 10^{-20}; T_{1/2} \sim 3$h.

^{235}U : $T_{1/2} = 26$ min; $E_\gamma = 76.5$ eV; $\Delta E_\gamma(\text{rec}) = 1.34 \cdot 10^{-8}$ eV (Mossbauer)
$\Delta E_\gamma(\text{rad}) = 2.9 \cdot 10^{-19}$ eV; $\Delta E_\gamma(\text{rad})/E_\gamma = \Delta\nu/\nu = 3.8 \cdot 10^{-21}$; $\Delta\nu = 7 \cdot 10^{-5}$ Hz.
$\beta(M4) \sim 10^{18}; \alpha(E3) \sim 10^{13}$

^{201}Hg : $T_{1/2} = 81$ ns; $E_\gamma = 1565$ eV; $\Delta E_\gamma(\text{rec}) = 6.54 \cdot 10^{-6}$ eV (Mossbauer)
$\Delta E_\gamma(\text{rad}) = 5.6 \cdot 10^{-9}$ eV; $\Delta E_\gamma(\text{rad})/E_\gamma = \Delta\nu/\nu = 3.6 \cdot 10^{-12}$; $\Delta\nu = 1.4 \cdot 10^6$ Hz.
$\beta(M1) \approx 3.0 \cdot 10^3; \alpha(E2) \approx 3.5 \cdot 10^7$

He-Neon (Iodine) laser gives $\Delta\nu/\nu \sim 10^{-11}$; $\lambda_{(\mathrm{He-Ne})}$=632.99139822 nm
Cesium laser gives $\Delta\nu/\nu \sim 10^{-13}$ to 10^{-14}; Atomic clock
Nuclear radiation provides stable frequency being not subjected by the external influence

THANK YOU FOR ATTENTION

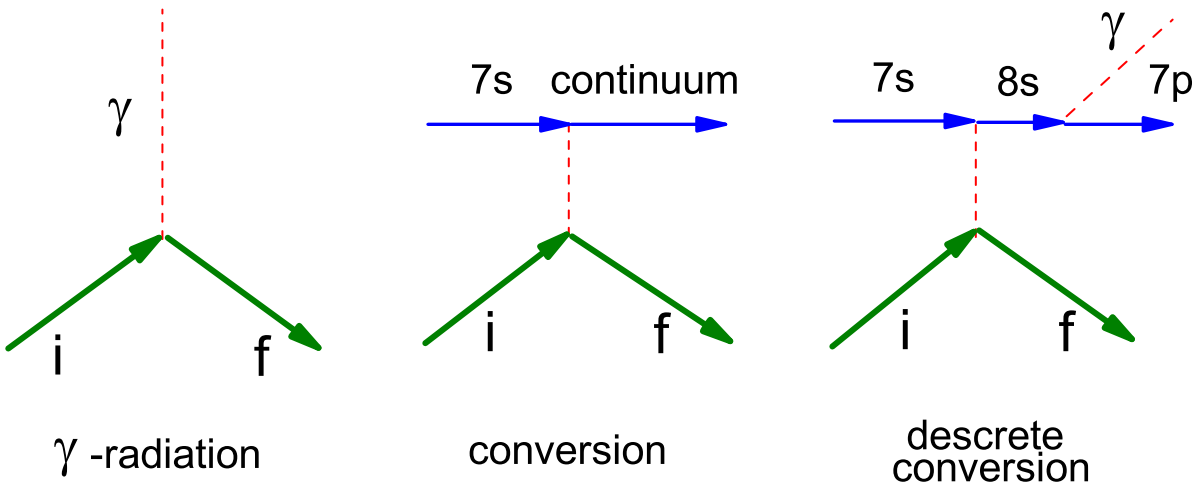

Figure 3: Diagrams showing γ-decay, conversion and descrete conversion